Available online at www.sciencedirect.com
ScienceDirect
Journal of the European Ceramic Society 29 (2009) 3167–3175
www.elsevier.com/locate/jeurceramsoc

Fabrication of yttria-stabilized-zirconia coatings using electrophoretic deposition: Effects of agglomerate size distribution on particle packing

Changzheng Ji, Ian P. Shapiro, Ping Xiao *

Materials Science Centre, School of Materials, University of Manchester, Grosvenor Street, Manchester M1 7HS, United Kingdom

Received 9 April 2009; received in revised form 12 May 2009; accepted 25 May 2009
Available online 27 June 2009

Abstract

Yttria-stabilized-zirconia (YSZ) particles with various size distributions have been electrophoretically deposited (EPD) on Fecralloy substrate to investigate the particle size effect on EPD coatings. The deposition rates, as-deposited particle packing densities, green densities and sintered (for 2 h at 1250 °C in air) coating hardnesses are dependent on particle size. The particle packing arrangement in EPD coatings can be affected by further electric field densification (EFD) of the as-deposited coating in which the wet EPD coating is immersed in pure solvent (acetylacetone) with the application of a constant electric field. The effect of EFD was found to be most effective on small particles (<0.5 μm) when they are co-deposited with large particles (>1 μm). The improvements are reflected in increased mechanical hardness of sintered coatings.

Keywords: A. Suspensions; A. Sintering; C. Hardness; D. ZrO_2; Packing

1. Introduction

Ceramic coatings on metallic substrates have many practical applications, e.g., for thermal protection,[1–3] wear and chemical resistance.[4] Plasma spraying, chemical vapour deposition and physical vapour deposition are currently common industrial practices, of which both the science and the technology have improved considerably.[5,6] However, they all have limitations for handling axially symmetric and complex-shaped substrates, and all three methods require expensive equipment, which makes them impractical for low-cost applications. Colloidal processing coating techniques, such as slurry/dip coating[7,8] and electrophoretic deposition (EPD),[9–12] provide the potential to fabricate a new generation of ceramic coatings with the advantages of less restriction in substrate shape, controlled chemical composition and microstructure, simple equipment requirements and low cost. As a colloidal coating-fabrication method, EPD has attracted increasing attention both academically and practically for its outstanding potential to tailor the microstructure and the thickness of ceramic coatings on complex-shaped substrates.[13,14]

In EPD, colloidal, charged particles deposit from a stable suspension onto an oppositely charged electrode (substrate) upon the application of a direct current electric field, and the wet deposit then undergoes drying and sintering to form the coating. The suspensions for EPD are prepared by dispersing particles in a liquid medium, of which the dispersion and stability can be achieved or enhanced by adjusting inter-particle forces.[15,16] The deposit weight and thickness can be controlled by EPD conditions, i.e. the properties of suspensions (particle concentration, viscosity, and electrical conductivity), deposition time and applied voltage.[10]

One of the most attractive features of EPD for fabricating advanced ceramic coatings is that microstructure can be controlled by manipulating the properties of the raw particles, i.e. the chemical composition, the crystal structure, the surface condition, and particle/agglomerate size.[10,16–18] It is commonly accepted that ceramic compacts with high green density and uniform, small pore size sinter most effectively.[19–21] Both experimental[22–24] and modelling[25,26] results on the effect of particle size on the compact density have suggested that bimodal or trimodal size mixtures provide higher green densities than uniform sized particles. McGeary[26] modelled the particle packing of the bimodal sized mixture and revealed that the maximum density is achieved when the size ratio (large to small) is greater than 7. These studies have led to the extensive use

* Corresponding author. Tel.: +44 161 200 5941; fax: +44 161 200 3586.
E-mail address: ping.xiao@manchester.ac.uk (P. Xiao).

0955-2219/$ – see front matter © 2009 Elsevier Ltd. All rights reserved.
doi:10.1016/j.jeurceramsoc.2009.05.032

of mixed size particles for achieving high density ceramics.[27] A controllable green density is desirable for EPD coatings, so the use of mixed sized particles to fabricate high green density EPD coatings should be investigated. The few studies specifically on the effect of particle size on the EPD process have only examined suspension stability,[28] electrophoretic mobility[29] and crack formation.[30] It is important to clarify the effect that particle size and shape have on the packing behaviour during EPD before optimising these to obtain high density coatings. In this work we investigate the effect of particle with various sizes but similar shapes.

In this study, yttria-stabilized-zirconia (8 mol.% $YO_{1.5}$, YSZ) particles were dispersed in acetylacetone to form stable suspensions, and EPD was carried out from these suspensions. The resulting EPD coatings were monitored by deposition efficiency and the particle packing density of wet coatings. EPD was carried out with the particles of varying size and size distribution and the effect on coating densities (wet, green and sintered) was examined. The particle packing of EPD coating under an electric field was also investigated by examining the effect of the electric field on properties of the coating after drying and sintering. The sintering behaviour of the EPD compacts, i.e. sintering shrinkage and microstructural development, was examined with the consideration of the substrate constraint effect.

2. Experimental procedure

2.1. Suspension preparation

Commercial 8 mol.% yttria-stabilized-zirconia (YSZ) particles (>99%, Pi-KEM, Shropshire, UK) with four different sizes, namely P0, P2, P5 and P10, were employed as raw particles. The suspension medium was acetylacetone (2,4-pentanedione, >99%, Sigma Aldrich Co. Ltd.). The suspension was prepared as follows: 2 g of YSZ particles was dispersed in 40 ml acetylacetone in a 50–ml glass beaker, followed by 300 s of ultrasonication using an ultrasonic probe (22.5 kHz, Microson XL 2000, Misonix Inc., Farmingdale, NY, USA). This resulted in a particle concentration of 50 kg/m^3 (volume concentration 0.83%). A field emission gun scanning electron microscope (10–20 kV, FEG-SEM, Philips XL-30, Eindhoven, Netherlands) was used to check the primary particle sizes, shapes and surface morphology of YSZ particles. The specific surface area of the YSZ particles was determined using a Brunauer–Emmett–Teller (BET) adsorption analyser (SA3100, Beckman-Coulter Inc., Fullerton, CA, USA) with nitrogen as adsorbant. The agglomerate size distribution of those suspensions was measured by laser light scattering (Mastersizer Micro Trac X100, Malvern, Worcestershire, UK) and the zeta potential of particles in acetylacetone was measured by a doppler electrophoretic light scattering analyzer (DELSA 440SX, Beckman-Coulter Inc., Fullerton, CA, USA).

A further investigation on the effects of particle size and size distribution during EPD was experimentally executed by EPD of centrifuge treated P5 suspension. 30 ml of P5 suspension was centrifuged for 120 s at either 800 or 2000 revolutions per minute (rpm). The resulting sediment and supernatant were separated, freeze dried and then re-dispersed in acetylacetone to prepare suspensions for EPD with narrower particle size distributions.

2.2. EPD of YSZ particles

Fresh, as-prepared suspensions were employed in the deposition experiments. A platinum sheet was used as the anode and a Fecralloy substrate (1 mm thick, Fe72.8/Cr22/Al5/Y0.1/Zr0.1 wt.%, GoodFellow, Cambridgeshire, UK), which had been polished down to 1 μm was used as the cathode. The two electrodes were set into the suspension vertically and parallel to each other with a separation of 10 mm, between which a voltage was applied (120 V). An electric field densification (EFD) treatment was applied to some samples immediately after the EPD process in an attempt to further improve the particle packing of the as-deposit coatings. EFD involved immersing the anode together with the coated cathode into pure acetylacetone solvent with an electric field (240 V) applied. A standard resistor (499 Ω) and a voltmeter were connected into the EPD circuit to detect the current flow during EPD and EFD. The wet coatings were then dried in an ambient atmosphere. All coatings were fabricated from freshly prepared suspensions, and for each EPD condition, at least 10 suspensions and 10 coatings were produced.

2.3. Characterization methods

The mass of as-deposited and dry coatings was measured (Ohaus AB-S, Leicester, UK). The deposit area of the coating was calculated by analyzing the image of the coatings taken by an optical microscope (Olympus BH, Tokyo, Japan). Hence the particle packing density of a wet coating ρ_w was calculated using the equation below:

$$\rho_w = \frac{m_d/\rho_{YSZ}}{((m_w - m_d)/\rho_{AcAc}) + (m_d/\rho_{YSZ})} \quad (1)$$

where m_w and m_d are the mass of wet and dry coating, respectively, and ρ_{YSZ} and ρ_{AcAc} are the theoretical density of fully dense YSZ (6.05×10^3 kg/m^3) and pure acetylacetone (0.98×10^3 kg/m^3), respectively. Green density ρ_d was measured and calculated by a mass and volume method:

$$\rho_d = \frac{m_d}{S\ d_d} \quad (2)$$

where d_d is the thickness of the green coating, which was measured by a magnetic thickness gauge (±2 μm, Ecotest Plus, Sheen Instruments, UK), and S is the deposit area. The green densities were obtained by taking the average value from 10 coatings fabricated under identical conditions. The results are reproducible to ±3%.

Dried green coatings were then removed from the substrates using a razor whilst maintaining the particle packing, and the free standing green bodies were heat treated in a furnace at 1250 °C for 2 h in air with a heating and cooling rate of 3 °C/min (CWF13/13, Carbolite, UK). The free sintered density was calculated using the in-plane shrinkage of the free standing coat-

ings by optical microscopy and image-analysis (ImageTools) of pieces of coatings before and after sintering. The linear in-plane sintering shrinkage ratio $\Delta L/L_0$ is defined as

$$\frac{\Delta L}{L_0} = \frac{L_0 - L_s}{L_0} \tag{3}$$

where L_0 and L_s are the lengths of the green coating and the sintered coating, respectively. The thickness shrinkage ratio due to sintering was calculated from the measured values of both green coating thickness d_d and freely sintered coating thickness d_{fs} using the thickness gauge. The free standing sintered density ρ_{fs} can be calculated from the following equation:

$$\rho_{fs} = \frac{\rho_d}{(1 - (\Delta L/L_0))^2 (d_{fs}/d_d)} \tag{4}$$

Adherent coatings were heat treated under the same sintering conditions as the free-standing green bodies. For constrained sintering, the coating can only shrink along the thickness direction, so the constrained sintered density ρ_{cs} can be calculated from the equation:

$$\rho_{cs} = \rho_d \frac{d_d}{d_{cs}} \tag{5}$$

where d_{cs} is the thickness of the constrained sintered coating measured by the thickness gauge.

Microstructures of sintered coatings were observed from the cross-sections of the coatings using FEG-SEM (as above). All samples had comparable thickness in the range of 100–170 μm. A thermally grown oxide (TGO) layer forms on the surface of Fecralloy during sintering both on exposed surfaces and beneath the YSZ coating. SEM-EDX shows the TGO to be an alumina layer less than 2 μm thick. The coating is well bonded to this TGO layer as is expected for a zirconia–alumina interface.

Mechanical hardness of sintered coatings was tested by indenting polished cross-sections using a micro-indentor (Vickers diamond indentor; Tukon 2100, Wilson Instruments, Norwood, MA, USA) under identical loading of 100 g force for all measurements. For each sample at least 10 valid indentations along the middle of the cross-section were averaged, the error bars (standard deviation) represent the variation between coatings.

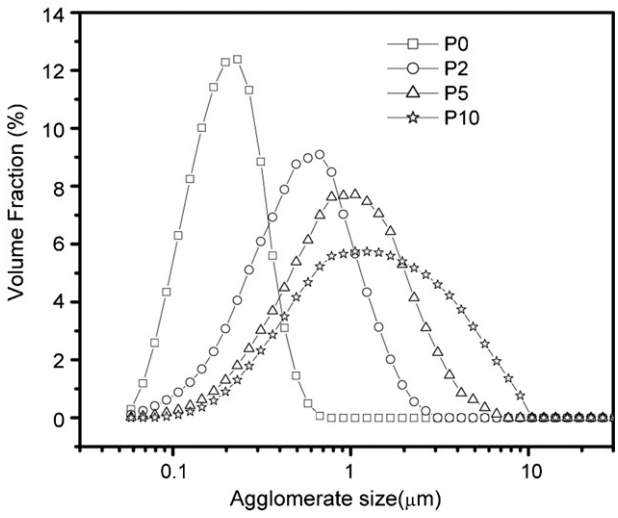

Fig. 1. Agglomerate size distributions of raw particles in acetylacetone suspension.

Table 1
BET surface area and quantified agglomerate size distribution of raw particles.

Particles	P0	P2	P5	P10
BET surface area (10^3 m^2/kg)	8.1	7.2	4.5	2.7
Maximum size a_{100} (μm)	0.6	2.0	5.0	10.0
Average size a_{50} (μm)	0.19	0.50	0.87	1.23
Standard deviation ($a_{8.41}/a_{50}$)	1.5	1.8	2.0	2.7

3. Results

3.1. Characterization of powders

The agglomerate size distributions are plotted for each batch of powder in Fig. 1. The BET surface area of those particles and quantified size distribution results are shown in Table 1.

The SEM image in Fig. 2a shows that P0 particles had spheroidal shapes and smooth surfaces with relatively uniform size. Fig. 2b shows that P10 particles have random shapes, as was the case for P2 and P5 powders. As shown in the higher magnification image at the top right-hand corner of Fig. 2b, large particles could be found, which have smooth surfaces. Significant ranges of particle size were observed for P2, P5 and

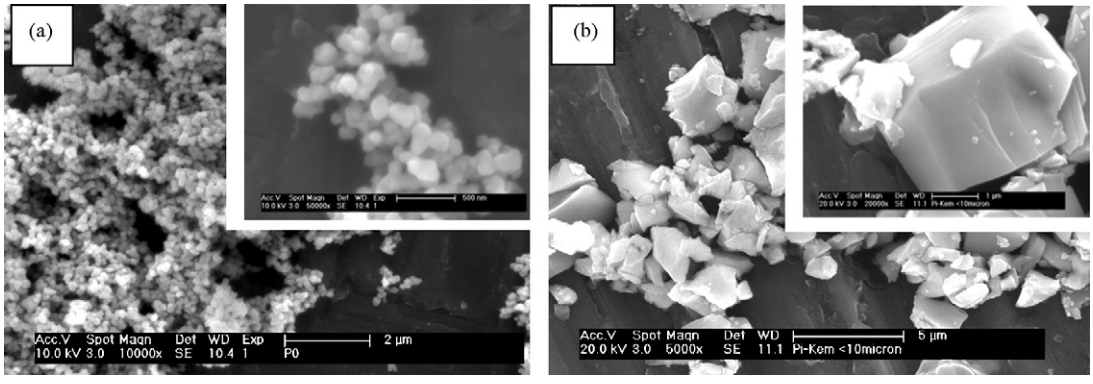

Fig. 2. SEM images which show the primary particle size, the particle shape and surface morphology of raw particles (a) P0 and (b) P10.

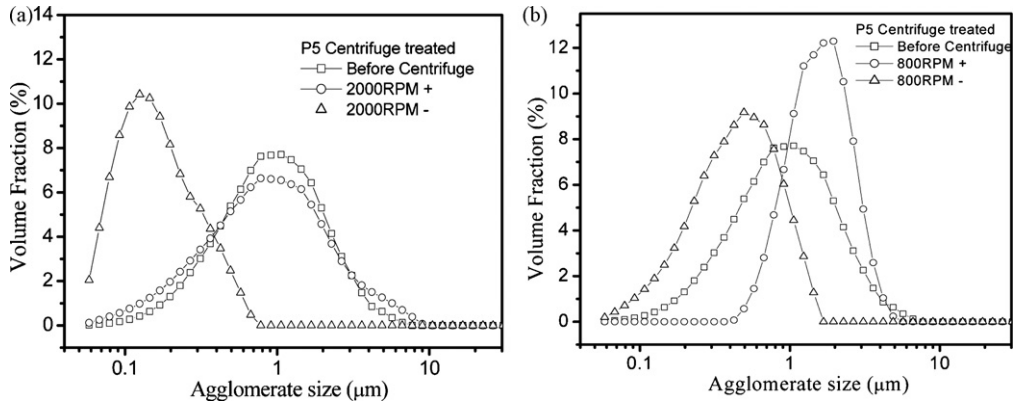

Fig. 3. Particle size distributions of centrifuge separated P5 powders at (a) 2000 rpm and (b) 800 rpm.

P10 powders, in which both small (<0.5 μm) and large (>1 μm) particles coexisted. These observations are consistent with the quantities given in Table 1.

Zeta potential of those particles in acetylacetone suspension was measured to be within a very narrow range (29.7 ± 0.3 mV) regardless of particle size, and hence was treated as constant.

Fig. 1 shows that all four batches of powder only P0 powder had relatively uniform size, whereas P2, P5 and P10 powders all showed non-uniform size distributions. Centrifuge treatment was carried out on P5 powder to narrow the particle size distribu-

Table 2
Agglomerate size and size distribution of centrifuge treated P5 powder.

Centrifuge treated powder	2000 rpm		800 rpm	
	P5−	P5+	P5−	P5+
Average size a_{50} (μm)	0.14	0.87	0.41	1.51
Standard deviation ($a_{84.1}/a_{50}$)	2.0	2.2	1.8	1.6
Mass ratio (%)	5.6	94.4	44.6	55.4

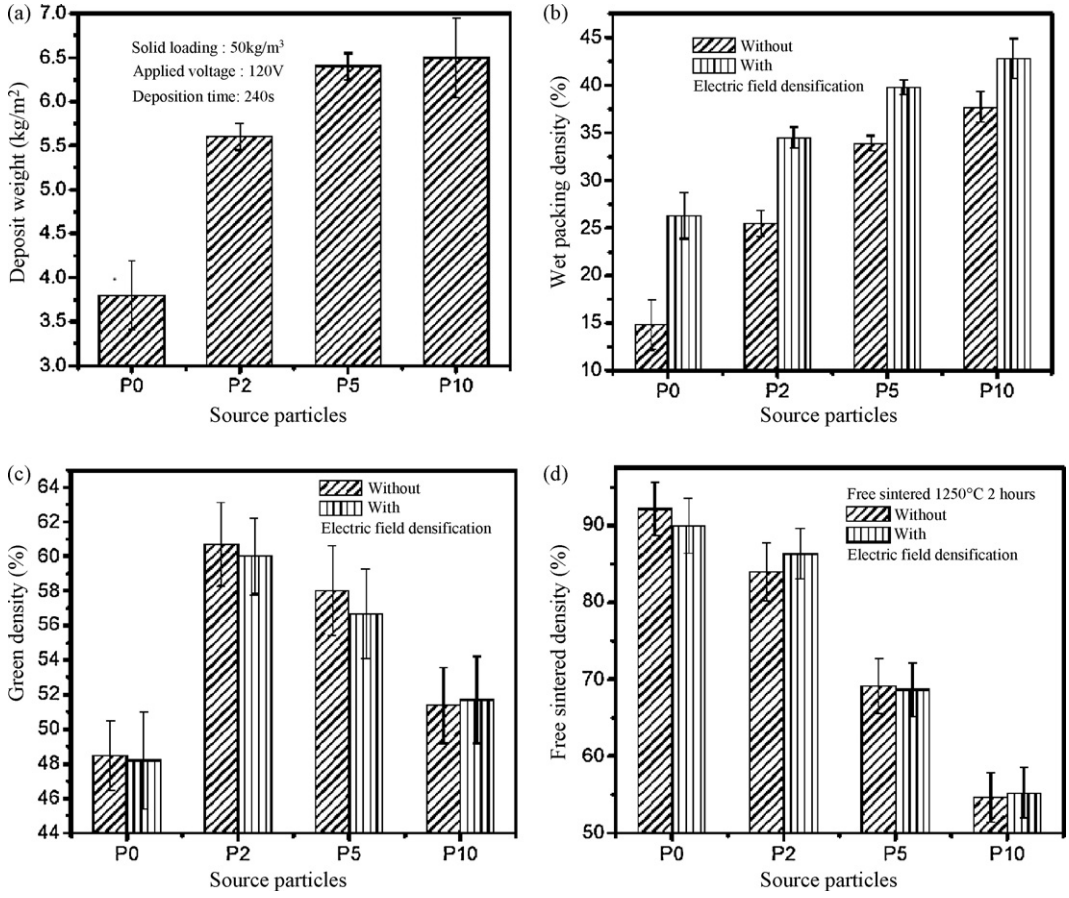

Fig. 4. EPD of different sized particles and effects of EFD on packing densities, (a) EPD deposit weight, (b) wet packing density, (c) green density, and (d) sintered density (free sintered at 1250 °C for 2 h).

tion. Centrifuge treated powder was separated into two groups of particles, relatively large particles (referred to as "+") contained in the sediment, and relatively small particles (referred to as "−") contained in the supernatant. Both high-speed (2000 rpm) and low-speed centrifugations (800 rpm) were used, and particle distribution of separated particles in comparison with the original particles is shown in Fig. 3 and Table 2.

3.2. Formation of EPD coatings

Larger particle sizes lead to a higher deposit weight for the same EPD conditions (Fig. 4a) and resulted in a higher wet coating density (Fig. 4b). The electric field densification (EFD) treatment increased the wet coating density (Fig. 4b) for all particles but the increase was most marked for small particles (P0 coatings increased from 14.8% to 26.3% wet density). For coatings with the largest particle size (P10 particles), the increase in the wet coating density due to the EFD was modest (from 37.7% to 42.8%). Fig. 4c shows the green densities of EPD coatings fabricated from the four batches of source particles. It can be seen from the diagram that coatings fabricated from particles with relatively broad size distributions, i.e. P2, P5 and P10 coatings, had higher green densities than P0 coatings, which had a uniform particle size. Free sintered coating densities were measured to further understand the effects of particle size on the microstructure of EPD coatings (Fig. 4d). Free sintered densities showed significant dependence on particle sizes, i.e. smaller particles provided higher sintered densities, as expected from classical sintering theory. The EFD had limited effect on green and free sintered coating densities despite the significant increase in wet coating density (Fig. 4b). However, there is an apparent effect of EFD on mechanical properties of EPD coating, which will be examined below.

SEM of sintered fracture surfaces (Fig. 5) showed different micro-packing structures for electric field densified coatings compared to coatings without this treatment. For P0 coatings, agglomerate like microstructures were found in coatings after the EFD, along with inter-agglomerate voids (Fig. 5b), which are attributed to differential sintering within the coating due to the uneven packing of particles. For P5 coatings, distinctive arrangements of smaller particles adhered to the surfaces of larger particles (Fig. 5d) were extensively observed in coatings with the EFD, which were also believed to be introduced by the EFD. The effects of these specific microstructures formed during EFD treatment have on the properties of EPD coatings are examined below.

3.3. Micro-hardness of free sintered EPD deposits

In this study, the micro-indentation hardness of free sintered coatings, under identical sintering conditions, was examined to help understand the effects of agglomerate size on the particle packing in EPD coatings and subsequent EFD and how this affects sintering.

Fig. 6 shows the hardness values of free sintered EPD coatings fabricated from particles with various agglomerate sizes. Coatings with larger particles had significantly lower hardness after sintering, which is consistent with classical sintering theory[31]

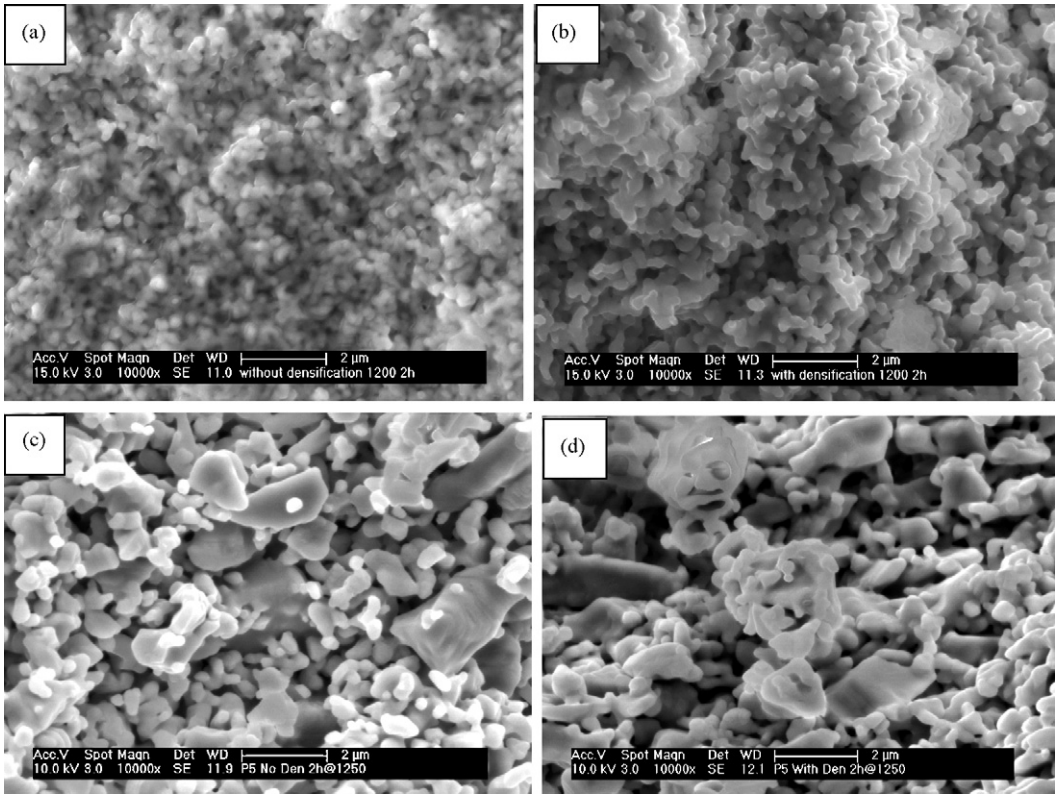

Fig. 5. SEM images of fracture surface of sintered coatings (a) P0 coating, (b) P0 coating with EFD treatment, (c) P5 coating, (d) P5 coating with EFD treatment.

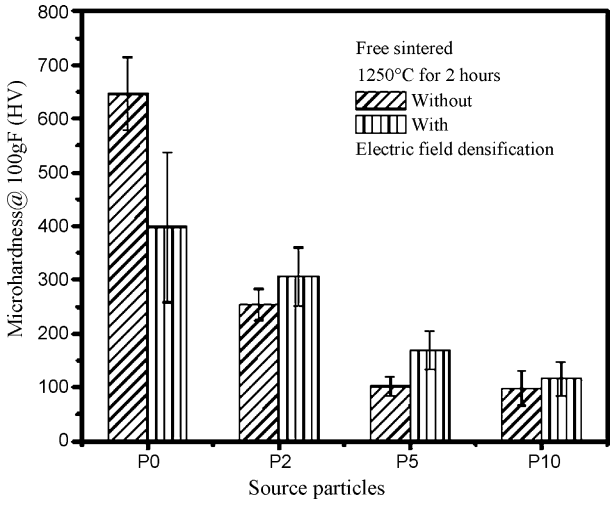

Fig. 6. Micro-hardness of free sintered EPD coatings fabricated with different sized particles.

in which large particles have lower sinterability than small particles.

The effect of the EFD process on the hardness of sintered coatings differed between powders. For P2, P5 and P10 coatings, the EFD increases the coating hardness (Fig. 6) despite having similar green and sintered densities for coatings with and without EFD (Fig. 4c and d). However, P0 coatings showed an opposite effect by the EFD. Hence the difference in hardness is attributed to the microstructure change during the EFD and will be discussed in Section 4.3.

3.4. EPD of centrifuge separated particles

By using the 800 rpm centrifuge treated P5 particles for EPD, the functions of both small and large sized particles on the microstructures of EPD coatings can be examined individually and compared to the original P5 coatings to further elucidate the EPD process in terms of deposition weight and particle packing.

Green densities (Fig. 7a) of coatings with mixed sized particles (P5 coatings) were higher than those of coatings fabricated from centrifuged particles (P5− coatings and P5+ coatings) with relatively narrow size distributions. No significant differences in green density were found between coatings with and without the EFD for P5− and P5+ coatings although there was a small increase for P5 coatings. Fig. 7b shows the hardness values of free sintered P5− and P5+ coatings, which indicated that the EFD gave less obvious effects on the hardness of sintered coatings for particles with relatively uniform size (P5− and P5+ particles) than those with broad size distributions (P5 particles). This phenomenon supports the previous result that the EFD treatment had positive effects on the particle packing only when coatings contained both large and small particles.

3.5. Constrained sintering of EPD coatings

Fig. 8a shows the green, free sintered and constrained sintered densities, of EPD coatings fabricated with various sized particles. The densities of free sintered coatings showed a large dependence on particle size, with increased particle size causing a significant decrease of the free sintered density. If we take the smallest and largest particles as examples, when the average particle size (a_{50}) increased from 0.19 μm (P0) to 1.23 μm (P10), the free sintered density decreased from 92.2% to 54.6%. When the coatings were sintered on the substrates, the sintered densities showed greater dependence on the green density. For instance, P0 coating presented 62.1% constrained sintered density because of its low green density (48.5%), whereas P2 coatings showed 67.4% constrained sintered density due to its high green density (60.7%). Fig. 8b shows the hardness of free and constrained sintered coatings with different sized particles. The hardness decreased when particle sizes increased for both sintering approaches, which indicated that large particles were hard to sinter and impart poor mechanical hardness to the coatings. The substrate constraint effect on hardness, which is shown by the difference in hardness between free and constrained sintered coatings, decreased with increasing particle size. For example, if we take the two extreme cases examined in this study, P0 (smallest) and P10 (largest): for P0 coatings the hardness decreased significantly from ~650 HV_{100gF} when free sintered to ~200 HV_{100gF} when constrained sintered, however, for P10 coatings the hardness changed only slightly from ~76 HV_{100gF} to ~40 HV_{100gF}.

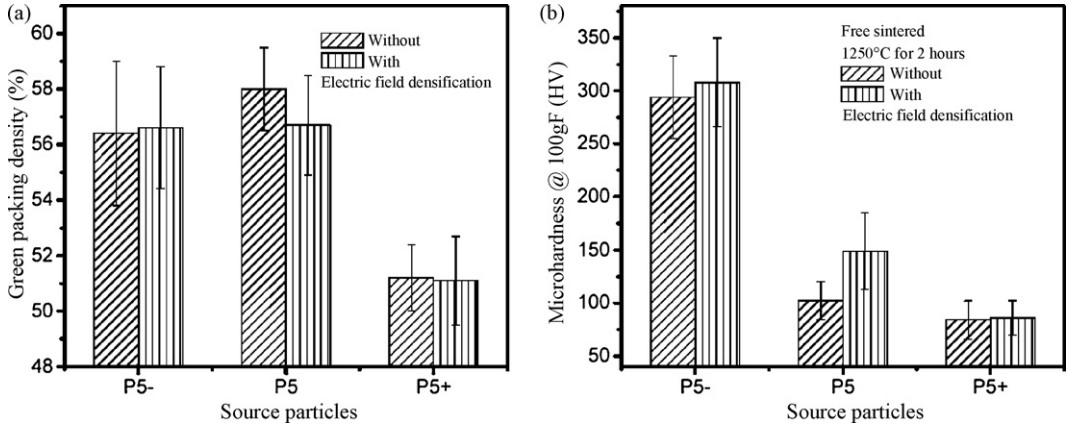

Fig. 7. EPD of centrifuge treated P5 particles (a) green densities and (b) micro-hardness of free sintered coatings.

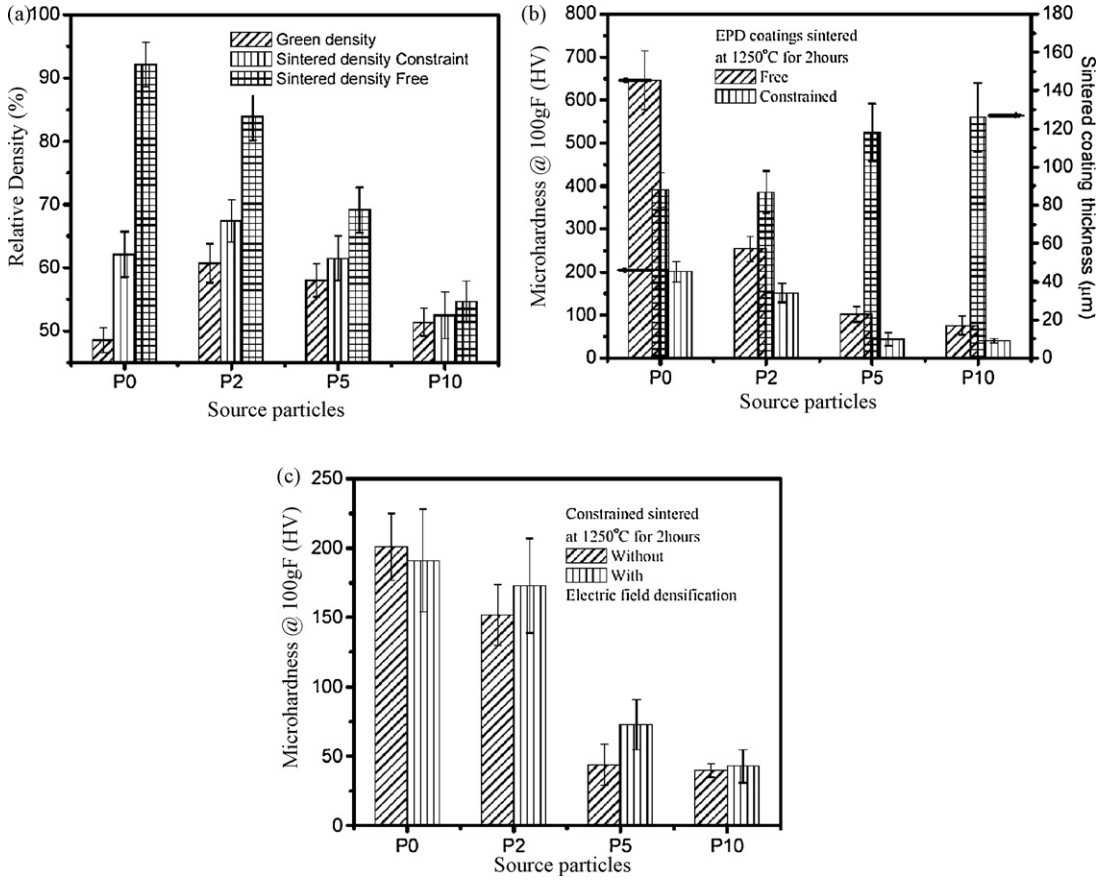

Fig. 8. Constrained sintered EPD coatings fabricated with different sized particles (a) coating densities (green, free sintered and constrained sintered), (b) micro-hardness, and (c) effect of the EFD on micro-hardness.

Fig. 8c shows that the effect of the EFD treatment on the micro-hardness of the constrained sintered coatings is quite different for different particles. For free sintered P0 coatings, the EFD made the coatings weaker than normal EPD coatings (Fig. 6), however when the coatings were sintered under constraint, the degrading effect caused by the EFD treatment was impaired. For P2 and P5 coatings, the EFD benefited the particle packing and improved the hardness of constrained sintered coatings as it did for free sintering. The EFD had little effect on the hardness of P10 coatings.

4. Discussion

4.1. Effect of agglomerate size distribution on EPD

Particle size had a marked effect on EPD kinetics with larger particles resulting in greater EPD efficiency despite having similar zeta potential (Fig. 4a).

Larger particle sizes also gave higher wet packing density (Fig. 4b). However the wet packing density did not appear to have a direct influence on the green density. The green density did strongly depend on agglomerate size distributions of the raw particles with a broad size distribution resulting in high green density. This result is consistent with previous work on the effect of particle size and size distribution on the packing densities of powder compacts in which small particles are able to fill the interstices between large particles.[23–27]

4.2. Sintered microstructure

In this work both constrained and free sintering were studied. The density obtained after free sintering is overwhelmingly influenced by particle size rather than green density, hence the density and hardness were greatest for P0 powders and least for P10. This trend is expected from classical sintering theory due to the reduced driving force for sintering of larger powders. The addition of sintering constraint restricts the degree of densification that occurs hence final sintered densities are lower for constrained sintered than for free sintered coatings. The substrate constraint retards the densification by two mechanisms: (1) the greater thermal expansion of the substrate ($11.1 \times 10^{-6}\,K^{-1}$ for Fecralloy[32]) compared to the ceramic coating ($7.7–9.6 \times 10^{-6}\,K^{-1}$ for YSZ[33]) exerts a tensile influence on the coating during the heating up period; (2) the rigidity of substrates during the isothermal stage, which constrains the in-plane shrinkage of the ceramic coating and leaves only one direction, the thickness, free to shrink. An effect of this reduced densification is to increase the significance of green density such that this becomes the dominant effect. The free sintered density can be considered as the limit which green samples move

towards as they sinter. The tensile constraining stress imposed by the substrate increases with sintering shrinkages (i.e. greater for easily sintered particles) such that these coatings remain further from their 'free sintered limit' and their initial green density becomes significant. In this manner, due to their reduced green density, constrained sintered coatings from P0 powders reached a lower final density than the coatings from P2 powders despite higher sinterability.

4.3. Electric field densification

The EFD treatment used in this work has a marked effect on the wet packing density of EPD coatings. However, as described above the wet packing density does not appear to influence the green density hence coatings made with and without the EFD treatment have similar green density.

The EFD treatment does, however, have subtle effects on the subsequent green microstructure which affects the sintering process such that the coating hardness is altered. In the case of P0 coatings the EFD treatment causes a dramatic reduction in the final free sintered hardness, which is as expected[34] for the agglomerate and inter-agglomerate void structure observed by SEM. Due to this dramatic effect of the EFD on P0 coatings the treatment is thought to affect the smallest particles most strongly. The EFD treatment might have caused agglomeration of the small particle fractions of P2, P5 and P10 coatings in the same way. These agglomerates may be with other small particles or between small and large particles. The effect of the EFD treatment was to improve the free sintered hardness of coatings made with P2, P5 and to a small extent P10 particles. SEM observation shows that after the EFD treatment small particles do stick to the surface of larger particles in coatings made from P2, P5 and P10 powders. Hence it is thought that the presence of small, more sinterable particles on the surface of large particles in these coatings act to form a bridge between large particles resulting in better sintering and greater hardness, compared to the coatings without the EFD where more large–large particle contacts exist which sinter poorly and restrict the strength of the coating. Where the particle size distribution was narrower, for example the centrifuge separated P5 powder, the EFD treatment had little effect on sintered hardness.

Microstructural differences are expected to have less effect on the hardness of constrained sintered coatings compared with free sintered coatings, as less densification occurs, in the same way that the effect of particle size on density was less significant when sintering constraint was introduced. This reduced densification can explain why the hardness of constrained sintered P0 coatings was only slightly degraded by the EFD treatment, rather than severely as was the case for free sintered coatings. However, the improvement in hardness due to EFD treatment of P2 and P5 particle coatings remained of similar magnitude when sintering was switched from free to constraint. The persistence of the effect of the EFD treatment is attributed to the important effect of necking between the large particles in these coatings. Even if the hardness is not improved due to increased density, increased strength of the connections between large particles, which are more commonly bridged by small particles after the EFD treatment, resulted in increased hardness for constrained sintered P2 and P5 coatings (Fig. 8c). The EFD had little effect on the hardness of P10 coatings, because these particles were so large that no matter what the particle packing little sintering occurred.

4.4. Deposition and packing mechanisms

The present results show that the EFD treatment after EPD can change the particle packing in the wet coatings (Fig. 4b), and has a significant impact on the hardness of the free-standing coatings (Fig. 6) although no significant changes to the green and free-standing coating densities (Fig. 4c and d) and constrained sintered coatings (Fig. 8c) were detected. So it is essential to make clear what happened during the EFD process.

Charged particles in suspension are surrounded by solvent molecules due to the existence of diffuse double layers, whose thickness, κ^{-1}, is dependent on the particle surface and the solvent. It has been reported by Sarkar and Nicholson[13,35] that free ions account for most of the charge transport during EPD and the particles coagulate on the electrode without necessarily losing all of their surface charge. Hence particles in the deposit are still surrounded by electric double layers, although the double layers may be depressed due to surface charge distortion in the electric field[13] and ionic depletion[36] in the vicinity of the electrode.

The retention of some surface charge in the deposit allows particles to continue moving after their first collision with the electrode or deposit. The influence of the electro-osmotic flow induced by the electric field[29,37,38] allows particles to rearrange themselves in the deposit. The ionic depletion near the electrode, together with the electro-osmotic flow during the EFD treatment, allows particles to rearrange to produce more inter-particle contacts.

5. Conclusions

Suspensions of YSZ powder with various particle size distributions in acetylacetone were prepared to study the particle sizes effects on the microstructural development of EPD coatings. Powders with non-uniform size distributions can be separated by centrifuge treatment of the suspension to obtain relatively uniformly sized particles.

The deposition rate, coating packing densities, including the wet density, green density and free sintered density, and the hardness of free sintered coatings showed direct dependence on the particle sizes. Mixed sized particles provide higher green density of EPD coatings than uniform sized particles as has previously been found for the compaction of dry powder. The density of sintered EPD coatings is determined by both green density and particle size, higher green density and smaller particle size leads to better sintered coatings. The improved sintering for smaller particles is reflected in harder coatings.

An EFD treatment in pure solvent after EPD increases the wet coating density due to the electro-osmotic flow within the coating and ionic depletion in the vicinity of the deposit electrode. The EFD is most effective in rearranging of smaller sized particles within the wet EPD coatings. The EFD changed the par-

ticle packing behaviour, i.e. the positions of small particles in the EPD coating, but had little effect on both green and sintered coating densities. However, the differences in particle packing caused by the EFD are detectable by examining the hardness of sintered coatings. Coatings fabricated with mono-sized small particles (P0) had reduced hardness after the EFD due to agglomeration of particles. However, when the EPD coating contained both small (P5−) and large (P5+) particles, the EFD increased the hardness of sintered coatings by arranging small particles to bridge between large particles and promote sintering.

Constrained sintered coatings showed lower density and hardness than free sintered coatings, and coatings made up of smaller particles were affected more by the substrate constraint during sintering because they had greater tendency to shrink than coatings containing larger particles. The EFD does not have a significant effect on the hardness of constrained sintered coating.

References

1. Clarke, D. R. and Levi, C. G., Materials design for the next generation thermal barrier coatings. *Ann. Rev. Mater. Sci.*, 2003, **33**, 383–417.
2. Evans, A. G., Mumm, D. R., Hutchinson, J. W., Meier, G. H. and Pettit, F. S., Mechanisms controlling the durability of thermal barrier coatings. *Prog. Mater. Sci.*, 2001, **46**, 505–553.
3. Padture, N. P., Gell, M. and Jordan, E. H., Thermal barrier coatings for gas-turbine engine applications. *Science*, 2002, **296**, 280–284.
4. Mayrhofer, P. H., Mitterer, C., Hultman, L. and Clemens, H., Microstructural design of hard coatings. *Prog. Mater. Sci.*, 2006, **51**, 1032–1114.
5. Choy, K. L., Chemical vapour deposition of coatings. *Prog. Mater. Sci.*, 2003, **48**, 57–170.
6. Mattox, D. M., Physical vapor deposition processes. *Prod. Finish.*, 2001, **65**(12), 72–82.
7. Lan, W. H., Wang, X. and Xiao, P., Agglomeration effect on drying of yttria-stabilised-zirconia slurry on a metal substrate. *J. Eur. Ceram. Soc.*, 2006, **26**(16), 3599–3606.
8. Lan, W. H. and Xiao, P., Constrained drying behaviour of yttria-stabilised-zirconia slurry on a substrate. I. Drying mechanism. *J. Am. Ceram. Soc.*, 2006, **89**, 1518–1522.
9. Ji, C., Lan, W. H. and Xiao, P., Fabrication of yttria-stabilized-zirconia coatings using electrophoretic deposition: packing mechanism during deposition. *J. Am. Ceram. Soc.*, 2008, **91**(4), 1102–1110.
10. Besra, L. and Liu, M., A review on fundamentals and applications of electrophoretic deposition (EPD). *Prog. Mater. Sci.*, 2007, **52**, 1–61.
11. Corni, I., Ryan, M. P. and Boccaccini, A. R., Electrophoretic deposition: from traditional ceramics to nanotechnology. *J. Eur. Ceram. Soc.*, 2008, **28**(7), 1353–1367.
12. Van der Biest, O. O. and Vandeperre, L. J., Electrophoretic deposition of materials. *Annu. Rev. Mater. Sci.*, 1999, **29**, 327–352.
13. Sarkar, P. and Nicholson, P. S., Electrophoretic deposition (EPD): mechanisms, kinetics and application to ceramics. *J. Am. Ceram. Soc.*, 1996, **79**, 1987–2002.
14. Boccaccini, A. R. and Zhitomirsky, I., Application of electrophoretic and electrolytic deposition techniques in ceramics processing. *Curr. Opin. Solid State Mater. Sci.*, 2002, **6**(3), 251–260.
15. Koelmans, H., Th, J. and Overbeek, G., Stability and electrophoretic deposition of suspensions in non-aqueous media. *Discuss Faraday Soc.*, 1954, **18**, 52–63.
16. Zhitomirsky, I., Cathodic electrodeposition of ceramic and organoceramic materials: fundamental aspects. *Adv. Colloid Interface Sci.*, 2002, **97**, 279–317.
17. Van der Biest, O. O., Joos, E., Vleugels, J. and Baufeld, B., Electrophoretic deposition of zirconia layers for thermal barrier coatings. *J. Mater. Sci.*, 2006, **41**, 8086–8092.
18. Wang, Z. C., Schemilt, J. and Xiao, P., Fabrication of ceramic composite coatings using electrophoretic deposition, reaction bonding and low temperature sintering. *J. Eur. Ceram. Soc.*, 2002, **22**(2), 183–189.
19. Ring, T. A., *Fundamentals Ceramic Powder Processing and Synthesis*. Academic Press, London, 1996.
20. Lewis, J. A., Colloidal processing of ceramics. *J. Am. Ceram. Soc.*, 2000, **83**(10), 2341–2359.
21. Lange, F. F., Powder processing science and technology for increased reliability. *J. Am. Ceram. Soc.*, 1989, **72**(1), 3–15.
22. Milne, S. J., Patel, M. and Dickinson, E., Experimental studies of particle packing and sintering behaviour of monosize and bimodal spherical particles. *J. Eur. Ceram. Soc.*, 1993, **11**, 1–7.
23. Hellmig, R. J. and Ferkel, H., Using nanoscaled powder as an additive in coarse-grained powder. *J. Am. Ceram. Soc.*, 2001, **84**(2), 261–266.
24. Messing Jr., G. L. and Onoda, G. Y., Inhomogeneity-packing density relations in binary powders. *J. Am. Ceram. Soc.*, 1978, **66**(1/2), 1–5.
25. Westman, A. E. R. and Hugill, H. R., Packing of particles. *J. Am. Ceram. Soc.*, 1930, **13**(10), 767–779.
26. McGeary, R. K., Mechanical packing of spherical particles. *J. Am. Ceram. Soc.*, 1961, **44**(10), 513–522.
27. Kong, C. M. and Lannutti, J. J., Agglomerate size distribution on loose packing fraction. *J. Am. Ceram. Soc.*, 2000, **83**(9), 2183–2188.
28. Hyam, R. S., Subhedar, K. M. and Pawar, S. H., Effect of particle size distribution and zeta potential on the electrophoretic deposition of boron films. *Colloids Surf. A*, 2008, **315**(1–3), 61–65.
29. Guelcher, S. A., Solomentsev, Y. and Anderson, J. L., Aggregation of pairs of particles on electrodes during electrophoretic deposition. *Powder Technol.*, 2000, **110**, 90–97.
30. Sato, N., Kawachi, M., Noto, K., Yoshinoto, N. and Yoshizawa, M., Effect of particle size reduction on crack formation in electrophoretically deposited YBCO films. *Physica C*, 2001, **357–360**, 1019–1022.
31. Kuang, X., Carotenuto, G. and Nicolais, L., A review of ceramic sintering and suggestions on reducing sintering temperatures. *Adv. Perform. Mater.*, 1997, **4**, 257–274.
32. Louro, C., Teixeira-Dias, F., Menezes, L. F. and Cavaleiro, A., Effect of the substrate thermal expansion coefficient on the thermal residual stresses in W–Si–N sputtered films. *Key Eng. Mater.*, 2002, **230–232**, 513–516.
33. Cai, P. Z., Green, D. J. and Messing, G. L., Constrained densification of alumina/zirconia hybrid laminates. I. Experimental observations of processing defects. *J. Am. Ceram. Soc.*, 1997, **80**(8), 1929–1939.
34. Rhodes, W. H., Agglomerate and particle size effects on sintering yttria-stabilized-zirconia. *J. Am. Ceram. Soc.*, 1981, **65**(1), 19–22.
35. De, D. and Nicholson, P. S., Role of ionic depletion in deposition during electrophoretic deposition. *J. Am. Ceram. Soc.*, 1999, **82**(11), 3031–3036.
36. Anne, G., Neirinck, B., Vanmeensel, K., Van der Biest, O. O. and Vleugels, J., Origin of the potential drop over the deposit during electrophoretic deposition. *J. Am. Ceram. Soc.*, 2006, **89**(3), 823–828.
37. Solomentsev, Y., Guelcher, S. A., Bevan, M. and Anderson, J. L., Aggregation dynamics for two particles during electrophoretic deposition under steady fields. *Langmuir*, 2000, **16**, 9208–9216.
38. Hoggard, J. D., Sides, P. J. and Prieve, D. C., Electrolyte-dependent multiparticle motion near electrodes in oscillating electric fields. *Langmuir*, 2008, **24**(7), 2977–2982.